

# Hetero-bichromophore Dyad as a Highly Efficient Triplet Acceptor for Polarity Tuned Triplet–Triplet Annihilation Upconversion

Ya Liu,<sup>†,‡</sup> Kepeng Chen,<sup>§</sup> Songqiu Yang,<sup>†</sup> Daoyuan Zheng,<sup>†,‡</sup> Guanghua Ren,<sup>†,‡</sup> Yang Yang,<sup>†,‡</sup> Jianzhang Zhao,<sup>§</sup> Donghui Wei,<sup>||</sup> and Keli Han<sup>\*,†,⊥</sup>

<sup>†</sup>State Key Laboratory of Molecular Reaction Dynamics, Dalian Institute of Chemical Physics, Chinese Academy of Sciences, 457 Zhongshan Road, Dalian 116023, People's Republic of China

<sup>‡</sup>University of Chinese Academy of Sciences, Beijing 100049, People's Republic of China

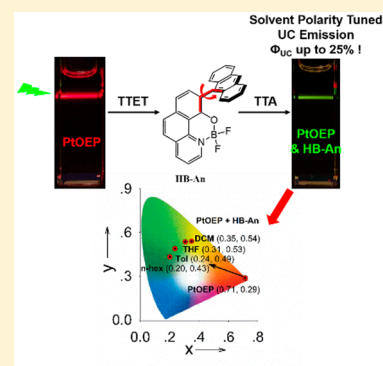
<sup>§</sup>State Key Laboratory of Fine Chemicals, School of Chemical Engineering, Dalian University of Technology, E-208 West Campus, 2 Ling Gong Road, Dalian 116024, People's Republic of China

<sup>||</sup>College of Chemistry and Molecular Engineering, Zhengzhou University, 100 Science Avenue, Zhengzhou 450000, People's Republic of China

<sup>⊥</sup>Institute of Molecular Sciences and Engineering, Shandong University, Qingdao 266000, People's Republic of China

## Supporting Information

**ABSTRACT:** Triplet–triplet annihilation upconversion (TTA UC) was intensively investigated for developing efficient photosensitizers and emitters. But an emission wavelength tunable TTA UC system with only one emitter was rarely reported. A novel hetero-bichromophore dyad, HB-An, showing solvatochromic emission and high fluorescence quantum yields in weakly polar solvents (such as *n*-hexane, dichloromethane (DCM), and so on) was used as triplet energy acceptor/emitter for polarity tuned TTA UC. A high TTA UC quantum yield up to 25% was achieved and the UC emission wavelengths can be fine-tuned from cyan to yellow by changing the media polarity. This information will be useful for constructing efficient emitting-light-tunable TTA UC system.



Photon upconversion by triplet–triplet annihilation with advantages of low excitation power and high quantum yields, has applications in organic light emitting diode,<sup>1,2</sup> photo(electro)chemistry,<sup>3–5</sup> solar cell devices,<sup>6–12</sup> and biological imaging.<sup>13,14</sup> The triplet–triplet annihilation upconversion (TTA UC) system is a bimolecular system, consisting of a sensitizer/triplet donor that can be optically or electrochemically pumped to its triplet state<sup>15–17</sup> and then triplet–triplet energy transfer (TTET) to a triplet acceptor/emitter undergoing TTA process that converts two lower-energy triplet excitons to one higher-energy singlet photon. The absorption and emission lights of the TTA UC system can be tuned by selecting the energy donor and acceptor independently,<sup>18</sup> but an emission wavelength tunable TTA UC system with only one emitter was rarely reported. To achieve this goal, the  $S_1$  state energy level of the emitter should be changeable by some external stimulus, such as surrounding polarity; meanwhile, the  $T_1$  state energy level remains unchanged.<sup>19</sup> In this principle, fluorescence chromophores with solvatochromic emissions are candidates for applications of solvent polarity tuned TTA UC. In recent years, a few bichromophore dyads based on polycyclic aromatic hydrocarbons (PAHs), such as anthracene, perylene, and their derivatives, were used as efficient triplet acceptors for improvement of TTA UC efficiency.<sup>20–22</sup> They

were constructed according to a principle that enlarging the driving force ( $2 \cdot E_{T_1} - E_{S_1}$ ) of the TTA process will improve the TTA UC efficiency. Although this design principle needs to be further verified, it was demonstrated that bichromophore dyads with appropriate energy levels are efficient triplet energy acceptors/annihilators. The hetero- or homo-bichromophore dyads, covalently linked by a single band, have long been reported about their fluorescence dependency on solvent polarity.<sup>21,23–27</sup> More importantly, the  $T_1$  state of multi-chromophore compounds always localized on one chromophore,<sup>28</sup> which makes the  $T_1$  state energy level independent of solvent polarity. However, just a few of them exhibit solvatochromic emission.<sup>23,25</sup> The relationship between molecular structure and the excited state properties is indistinct. Moreover, electron transfer between the two chromophores frequently decreases the fluorescence intensity even in weakly polar solvents,<sup>25</sup> which is harmful to overall upconversion efficiency. Therefore, it is meaningful to explore new bichromophore emitters with appropriate energy levels

Received: May 21, 2019

Accepted: July 16, 2019

Published: July 16, 2019

and solvatochromic emissions for constructing efficient emission wavelength tunable TTA UC system.

Herein, a novel hetero-bichromophore dyad, HB–An, linked by a single bond, showing solvatochromic emission and high fluorescence quantum yields in weakly polar solvents, was constructed (Figure 1a). The  $S_1$  state energy levels of the HB–

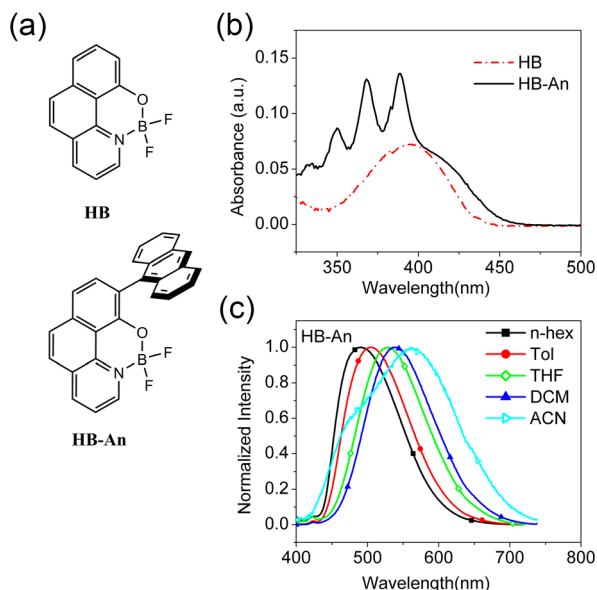


**Figure 1.** (a) Molecular structures of the HB–An dyad and the reference compound HB. (b) UV–vis absorption spectra in dichloromethane,  $c = 1.0 \times 10^{-5}$  M, 20 °C. (c) Normalized fluorescence spectra of HB–An in different solvents.  $\lambda_{\text{ex}} = 375$  nm. The absorbance of all samples at 375 nm is 0.03, 20 °C.

An dyad are much lower than that of anthracene (3.31 eV), meanwhile the  $T_1$  state energy level remains unchanged compared to that of anthracene. When the HB–An dyad was used as triplet acceptor/emitter for TTA UC, high TTA upconversion quantum yield, up to 25%, was achieved and the UC emission wavelengths can be fine-tuned by the media polarity.

The HB moiety is a  $\text{BF}_2$ -rigidified fluorophore, showing large Stokes shift ( $\sim 77$  nm) and full width at half-maximum (fwhm, ca. 118 nm) (Figure S8). The absorption bands of the HB–An dyad are a superposition of equivalent anthracene and HB compound and show no solvent polarity dependency (Figure S9). However, slight splitting of the primary absorption band at 425 nm indicates minimal electron coupling between the HB moiety and the anthracene unit at the ground state (Figure 1b).<sup>25</sup> This was supported by density functional theory (DFT) geometry optimization of the HB–An dyad, which showed that the dihedral angle between the HB and anthracene moieties is  $66^\circ$  at the ground state. On the contrary, the fluorescence emission is dramatically influenced by solvent polarity. With increasing solvent polarity, a pronounced bathochromic shift was observed (Figure 1c). Large Stokes shift and fwhm were also observed for the HB–An dyad.

Nanosecond transient absorption spectra (ns TAS) of the HB–An dyad in solvents with different polarities were performed to investigate the solvent effect of its triplet state. The ns TAS features of the dyad in toluene, dichloromethane (DCM), and acetonitrile (ACN) are similar and exhibit an

excited state absorption (ESA) signal peaked at 430 nm corresponding to  $T_1$  state absorption (Figure S10). This is a feature of anthracene chromophore TAS<sup>29</sup> and is totally different from the HB compound nanosecond transient absorption signal (Figure S11), indicating that the  $T_1$  state is populated and localized on the anthracene moiety ultimately. With a localized electron distribution, the  $T_1$  state energy level of the HB–An dyad is not sensitive to solvent polarity. The long triplet state lifetime is also essential for TTA UC triplet acceptor. The triplet state lifetime of the HB–An dyad is 358  $\mu\text{s}$  in toluene and 219  $\mu\text{s}$  in DCM (Figure S10d and S10e), which is sufficiently long for diffusion controlled intermolecular collision in TTET and TTA upconversion process.

The HB–An dyad was used as triplet acceptor/emitter for constructing a solvent polarity tuned TTA UC system; metalloporphyrin PtOEP (platinum octaethylporphyrin), the traditionally used triplet state energy donor for anthracene derivatives with a Q-band absorption peaked at 535 nm and a triplet energy level of 1.91 eV was used as photosensitizer.<sup>30–32</sup> The TTA UC system was excited by a 532 nm continuum light with a power of 74 mW/cm<sup>2</sup>, and the emission spectra in four solvents are given in Figure 2a. When the acceptor, the HB–

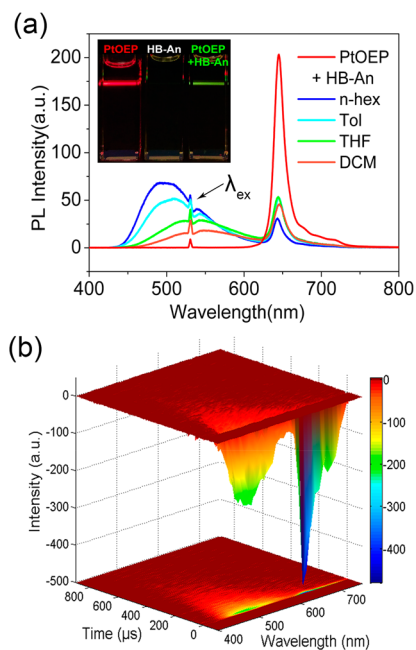


**Figure 2.** (a) Upconversion emission of the HB–An dyad in deaerated solvents. PtOEP was used as the sensitizer. Inset: photographs of PtOEP alone, HB–An alone, and the upconversion of the HB–An dyad in deaerated toluene.  $\lambda_{\text{ex}} = 532$  nm (74 mW/cm<sup>2</sup>). (b) Time-resolved emission spectra (TRES) of the TTA upconversion system in deaerated toluene (532 nm, 6.0 mJ/pulse).  $c(\text{PtOEP}) = 5.0 \times 10^{-6}$  M,  $c(\text{HB–An}) = 6.0 \times 10^{-5}$  M, 20 °C.

An dyad, was added, the red phosphorescence of PtOEP disappeared, but instead intense upconverted fluorescence emission of the HB–An dyad was observed. The most intense emission was observed in *n*-hexane with a high upconversion quantum yield of 25% at this condition. The upconverted emissions are red-shifted with increasing solvent polarity and the emission intensities decreased simultaneously, which is correlative with the fluorescence quantum yields of the HB–An dyad in these solvents (Table S2). It should be mentioned that part of the UC emission band of the TTA UC system in

tetrahydrofuran (THF) and DCM are down-converted when excited by 532 nm light. This is the restriction of the excitation light source available for the lab, but not a limitation of the TTA UC system. More importantly, the UC emission bands in THF and DCM were adopted to illustrate the tendency of emission wavelength change with increasing solvent polarity. The UC emission intensity, that is, the  $\Phi_{uc}$ , depends on the HB–An concentration. When the concentration of the HB–An dyad increased to  $6 \times 10^{-5}$  M, the  $\Phi_{uc}$  reached the highest in respective solvents. The  $\Phi_{uc}$  will no longer improve and will even decrease when the HB–An concentration continuously increases (Figure S12). The phenomenon of “increase–decrease” (first increase and then decrease) of  $\Phi_{uc}$  along with increasing acceptor concentration has been reported before.<sup>33,34</sup> The dependence of UC emission intensity on excitation power was also investigated and an excitation power of 74 mW/cm<sup>2</sup> above the threshold power  $I_{th}$  was adopted for an efficient TTA process (Figure S13).<sup>35</sup>

The quenching of phosphorescence of PtOEP and the rise of a long lifetime emission of the HB–An dyad upon 532 nm excitation was also observed in the time-resolved emission spectra (TRES) of the TTA UC system in deaerated toluene (Figure 2b), which demonstrated that TTET between PtOEP and the HB–An dyad happened and the upconverted emission of the TTA UC system is delayed fluorescence, which has a lifetime of 77.3  $\mu$ s in toluene (Figure S14). In order to investigate the TTET process efficiency between PtOEP and the HB–An dyad, Stern–Volmer quenching curves of PtOEP triplet state lifetimes vs concentrations of the HB–An dyad were plotted in *n*-hexane and toluene whose viscosities are very different (Figure S15). The quenching results demonstrated that the TTET quantum yields were both over 90% under the experimental conditions, with a bimolecular quenching constant of  $1.1 \times 10^{10}$  s<sup>−1</sup> in *n*-hexane and  $5.3 \times 10^9$  s<sup>−1</sup> in toluene (Table S2).

The mechanism of solvatochromic emission of the HB–An dyad is important for developing a new family of TTA UC emitters. The property of the excited state responsible for the emission is not the same for all solvents. In weakly polar solvents (such as *n*-hexane, toluene, THF and DCM), a moderate to strong fluorescence with  $\Phi_F \geq 0.6$  and single-exponential fluorescence decay (6.3 ns in *n*-hexane and 8.2 ns in DCM) was observed (Figure S16a and Table S1), which indicated that the lowest excited state is a solvent relaxed  $S_1$  ( $R_{S_1}$ ) state, whose dipolar moment is larger than the ground state.<sup>19</sup> In highly polar solvents, such as acetonitrile and DMSO, the fluorescence was almost completely quenched (Figure S9). Two emission bands peaked at 475 and 562 nm were observed. Both of the emission bands exhibit a double-exponential fluorescence decay: a short-lived component (2.2 ns) is dominant at 566 nm, and a long-lived component (6.9 ns) is dominant at 475 nm (Figure S16b and Table S1). These results indicated that full charge separation may be formed in highly polar solvents, where the emission band peaked at 562 nm represents the charge transfer (CT) state and the emission band peaked at 475 nm represents a local excited (LE) state possessing different geometry from the CT state. Generally, the LE state is an electron localized state upon excitation and is not sensitive to the solvent effect, but the CT state is opposite. There will be a charge shift in the CT state resulting in a large dipolar moment that interacts with polar solvent molecules to reduce the energy of the excited state.<sup>19</sup>

What is the reason for the large dipolar moment of the relaxed  $S_1$  state and CT state upon excitation of the HB–An dyad? We suspected that there is a twisting between the HB and anthracene units since the steric hindrance is small, which is analogous to twisted internal charge transfer (TICT).<sup>36</sup> Luminescence spectra of the HB–An dyad in DCM and ACN at 77 K were performed (Figure S17). Both of the spectra at 77 K showed a strong emission peaked at 475 nm, which is coincident with the LE state emission of the HB–An dyad in ACN at room temperature. This result demonstrated that there is a molecular geometry change or twisting at the relaxed  $S_1$  state and the CT state compared to the ground state structure, and the 475 nm emission band in ACN is attributed to LE state without molecular geometry change upon excitation. The DFT/time-dependent (TD)-DFT calculation results showed more. The optimized ground state and excited state geometries showed that the dihedral angle between the HB and the anthracene units twisted from  $\sim 66^\circ$  at the ground state to  $\sim 59^\circ$  at the  $S_1$  state, which could lead to an increase in electron coupling at the excited state (Table S3). When considering the molecular orbitals and configurations involved in the excited states, the  $S_1$  state is dominated by a HOMO  $\rightarrow$  LUMO transition with electron transfer from the anthracene unit to the HB moiety, the  $S_2$  state is dominated by a HOMO  $\rightarrow$  LUMO+1 transition in which electron is localized at the anthracene unit (Figure S20). In *n*-hexane and DCM, the relaxed  $S_1$  state can be described as hybridization of the optimized  $S_1$  state and  $S_2$  state; that is, the relaxed  $S_1$  state contains charge separation (CS) and LE components simultaneously.<sup>37</sup> Some researchers named it the “hybridized local and charge transfer” (HLCT) state.<sup>38</sup> In ACN, the CT state is the  $S_1$  state, and the LE state possessing a ground state geometry can be described by  $S_0 \rightarrow S_1$  vertical excitation with an energy level of 2.58 eV, which is in accord with the steady state fluorescence spectra. All of these results demonstrated that the increased electron coupling and geometry relaxation of HB–An lead to a considerable increase in excited state polarization and bathochromic emission from the LE state, which is responsible for the solvatochromism of the fluorescence emission of the HB–An dyad.

$$\Phi_{UC} = \Phi_{ISC} \times \Phi_{TTET} \times \Phi_{TTA} \times \Phi_F \quad (1)$$

The overall TTA UC efficiency can be evaluated by eq 1. The nonradiative decay of the relaxed  $S_1$  state of the HB–An dyad in weakly polar solvents competes with fluorescence and then restricts the overall  $\Phi_{uc}$ . But, ns TAS of HB–An showed that  $T_1$  state was formed upon photoexcitation. Formation of the  $T_1$  state via intersystem crossing (ISC) from the  $S_1$  state can feed back to the TTA process, which will break the restriction of  $\Phi_F$ . The optical density (OD) values of the ESA signal in ns TAS directly related to the triplet quantum yield of the HB–An dyad are largest in DCM (Figure S10), which is in agreement with the results obtained from singlet oxygen quantum yield ( $\Phi_\Delta$ ) measurement (Table S1). That is, in weakly polar solvents, the fluorescence quantum yields decrease; meanwhile, the triplet state quantum yields increase with increasing solvent polarity. These results indicated that the nonradiative deactivation path of the relaxed  $S_1$  state is ISC to the  $T_1$  state.

This was demonstrated by fs TAS in toluene (Figure 3). With a formation time of 1.5 ns, the EAS signal peaked at ca. 455 nm shifted to ca. 430 nm, corresponding to absorption of the triplet excited state. Therefore, the ISC process was



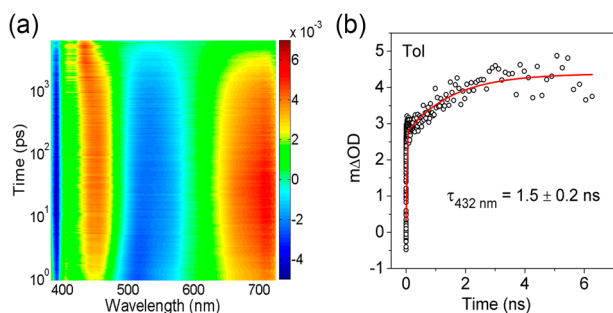


**Figure 3.** Femtosecond transient absorption spectra of HB-An in Tol ( $\sim 200 \mu\text{M}$ ) upon excitation at 370 nm using an excitation power of 40 nJ/pulse. (a) Contour plot of the femtosecond TAS. (b) Kinetic traces registered at 432 nm.

visualized by this peak shift, and the EAS signals peaked at 455 and 700 nm are assigned to the relaxed  $S_1$  state absorption of the HB-An dyad with a formation rate of  $2.0 \times 10^{11} \text{ s}^{-1}$ . The negative band peaked at 510 nm corresponds to the stimulated emission (SE) signal of the HB-An dyad. Similar results were observed in DCM (Figure S18). The formation rate of the relaxed  $S_1$  state is  $3.5 \times 10^{11} \text{ s}^{-1}$ . The following ESA signal blue shift to ca. 430 nm representing triplet state formation was also observed, with an ISC rate of  $5.9 \times 10^8 \text{ s}^{-1}$  in DCM. The mechanism of the ISC process of the HB-An dyad in weakly polar solvents is indistinct. ISC from the CT state to the  $T_1$  state was also observed for the HB-An dyad in ACN, whose mechanism is attributed to spin-orbital charge transfer induced ISC (SOCT-ISC) which was extensively accepted for donor-acceptor complexes.<sup>26</sup> But most of them non-radiatively decay to the ground state by charge recombination. Overall, a simplified Jablonski diagram is proposed to summarize the obtained results (Figure 4).

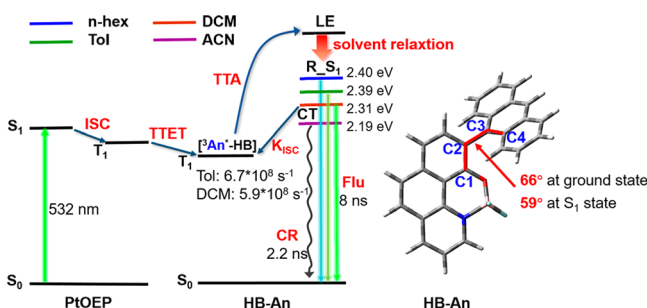


**Figure 4.** Illustrative diagram of the TTA UC process between PtOEP and the HB-An dyad.

In conclusion, we have constructed a hetero-bichromophore dyad, HB-An, showing solvatochromic emission. The HB-An dyad was used as an emitter/triplet acceptor for application of solvent polarity tuned TTA UC with PtOEP as photosensitizer. With excitation by 532 nm light with a power density of  $74 \text{ mW/cm}^2$ , high TTA upconversion quantum yields up to 25% were achieved. Moreover, the upconversion emission wavelength of the TTA UC system can be fine-tuned from cyan to yellow by changing the polarity of the solvents. Steady state, time-resolved spectra and DFT/TD-DFT calculations showed that geometry relaxation and increased electron coupling of the HB-An dyad at the excited state are responsible for the solvatochromic emission of the HB-An dyad. This information will be useful for developing a new family of TTA UC

emitters to construct efficient emitting-light-tunable TTA UC system. Furthermore, the HB-An dyad displays strong green light emission in the aggregated state (Figure S19), which can serve as an attractive emitting light material. The polarity changing strategy may perhaps also be applied to the polymer matrix for potential applications in the photoelectric field.

## EXPERIMENTAL METHODS

**General Information.** All the chemicals and solvents used in synthesis are analytically pure and were used as received. Steady state UV-vis absorption spectra were registered on a PerkinElmer Lambda35 spectrophotometer. Steady state photoluminescence spectra were measured on a Horiba Jobin Yvon FluoroMax-4 spectrofluorometer. The time-resolved fluorescence decays were recorded on a HORIBA Jobin Yvon TCSPC lifetime system, and the data analysis was conducted via commercial software provided by Horiba Instruments.

**Ultrafast Transient Absorption Spectroscopy.** Nanosecond transient absorption spectra were recorded on a homemade pump-probe setup with an apparatus response time of 20 ns. All the samples were thoroughly degassed via nitrogen bubbling for 15 min. Femtosecond transient absorption measurements were recorded on a homemade pump-probe laser system based on a regenerative amplified Ti:sapphire laser oscillator system from Coherent (800 nm, 35 fs, and 1 kHz repetition rate). Excitation pulses at 370 nm is obtained by pumping a TOPAS optical parametric amplifier (OPA) by a portion of the fundamental 800 nm. The polarization of the pump pulse was set to the magic angle ( $54.7^\circ$ ) relative to the probe pulse. A broad-band white light continuum generated by a CaF2 window (380–730 nm) was used as the probe beam. The delay between the pump and probe pulses was controlled by a motorized delay stage. Transient spectra were acquired in a time interval spanning up to 8 ns. Measurements were carried out in a quartz cell (1 mm thick) at room temperature.

**Hazards.** No unexpected or unusually high safety hazards were encountered in the course of this work.

## ASSOCIATED CONTENT

### Supporting Information

The Supporting Information is available free of charge on the ACS Publications website at DOI: 10.1021/acs.jpclett.9b01454.

Molecule synthesis and characterization, NMR spectra, fluorescence quantum yield experimental details, absorption and fluorescence spectra, dependence of upconversion quantum yields on the concentration, dependence of upconverted emission intensity on the excitation power density, decay trace of the TRES of HB-An, Stern-Volmer plot, fluorescence lifetime plots, table of photophysical and upconversion parameters, and DFT/TD-DFT calculation details, electron density maps, table of excitation energies and oscillator strengths (PDF)

## AUTHOR INFORMATION

### Corresponding Author

\*klhan@dicp.ac.cn.

### ORCID

Yang Yang: 0000-0002-3387-2417

Jianzhang Zhao: 0000-0002-5405-6398

Donghui Wei: 0000-0003-2820-282X

Keli Han: 0000-0001-9239-1827

## Notes

The authors declare no competing financial interest.

## ACKNOWLEDGMENTS

This paper is dedicated to the 70th anniversary of the Dalian Institute of Chemical Physics, Chinese Academy of Sciences. We are grateful to the National Natural Science Foundation of China (Grant Nos: 21533010 and 21833009), the National Key Research and Development Program of China (Grant 2017YFA0204800), DICP DMT0201601, DICP ZZBS201703, and the Science Challenging Program (JCKY2016212A501).

## REFERENCES

- (1) Chen, Y. H.; Lin, C. C.; Huang, M. J.; Hung, K.; Wu, Y. C.; Lin, W. C.; Chen-Cheng, R. W.; Lin, H. W.; Cheng, C. H. Superior Upconversion Fluorescence Dopants for Highly Efficient Deep-Blue Electroluminescent Devices. *Chem. Sci.* **2016**, *7*, 4044–4051.
- (2) Lin, B.-Y.; Easley, C. J.; Chen, C.-H.; Tseng, P.-C.; Lee, M.-Z.; Sher, P.-H.; Wang, J.-K.; Chiu, T.-L.; Lin, C.-F.; Bardeen, C. J.; Lee, J.-H. Exciplex-Sensitized Triplet–Triplet Annihilation in Heterojunction Organic Thin-Film. *ACS Appl. Mater. Interfaces* **2017**, *9*, 10963–10970.
- (3) Khnayzer, R. S.; Blumhoff, J.; Harrington, J. A.; Haefele, A.; Deng, F.; Castellano, F. N. Upconversion-Powered Photoelectrochemistry. *Chem. Commun.* **2012**, *48*, 209–211.
- (4) Kim, J.-H.; Kim, J.-H. Encapsulated Triplet–Triplet Annihilation-Based Upconversion in the Aqueous Phase for Sub-Band-Gap Semiconductor Photocatalysis. *J. Am. Chem. Soc.* **2012**, *134*, 17478–17481.
- (5) Lin, B.-Y.; Easley, C. J.; Chen, C.-H.; Tseng, P.-C.; Lee, M.-Z.; Sher, P.-H.; Wang, J.-K.; Chiu, T.-L.; Lin, C.-F.; Bardeen, C. J.; Lee, J.-H. Exciplex-Sensitized Triplet–Triplet Annihilation in Heterojunction Organic Thin-Film. *ACS Appl. Mater. Interfaces* **2017**, *9*, 10963–10970.
- (6) Schulze, T. F.; Cheng, Y. Y.; Fückel, B.; MacQueen, R. W.; Danos, A.; Davis, N. J. L. K.; Tayebjee, M. J. Y.; Khoury, T.; Clady, R. G. C. R.; Ekins-Daukes, N. J.; Crossley, M. J.; Stannowski, B.; Lips, K.; Schmidt, T. W. Photochemical Upconversion Enhanced Solar Cells: Effect of a Back Reflector. *Aust. J. Chem.* **2012**, *65*, 480–485.
- (7) Börjesson, K.; Dzebo, D.; Albinsson, B.; Moth-Poulsen, K. Photon Upconversion Facilitated Molecular Solar Energy Storage. *J. Mater. Chem. A* **2013**, *1*, 8521–8524.
- (8) Nattestad, A.; Cheng, Y. Y.; MacQueen, R. W.; Schulze, T. F.; Thompson, F. W.; Mozer, A. J.; Fückel, B.; Khoury, T.; Crossley, M. J.; Lips, K.; Wallace, G. G.; Schmidt, T. W. Dye-Sensitized Solar Cell with Integrated Triplet–Triplet Annihilation Upconversion System. *J. Phys. Chem. Lett.* **2013**, *4*, 2073–2078.
- (9) de Wild, J.; Meijerink, A.; Rath, J. K.; van Sark, W. G. J. H. M.; Schropp, R. E. I. Upconverter Solar Cells: Materials and Applications. *Energy Environ. Sci.* **2011**, *4*, 4835–4848.
- (10) Schulze, T. F.; Schmidt, T. W. Photochemical Upconversion: Present Status and Prospects for Its Application to Solar Energy Conversion. *Energy Environ. Sci.* **2015**, *8*, 103–125.
- (11) Pedrini, J.; Monguzzi, A. Recent Advances in the Application Triplet–Triplet Annihilation-Based Photon Upconversion Systems to Solar Technologies. *J. Photonics Energy* **2018**, *8*, 1–16.
- (12) Monguzzi, A.; Borisov, S. M.; Pedrini, J.; Klimant, I.; Salvalaggio, M.; Biagini, P.; Melchiorre, F.; Lelii, C.; Meinardi, F. Efficient Broadband Triplet–Triplet Annihilation-Assisted Photon Upconversion at Subsolar Irradiance in Fully Organic Systems. *Adv. Funct. Mater.* **2015**, *25*, 5617–5624.
- (13) Kwon, O. S.; Song, H. S.; Conde, J.; Kim, H.-i.; Artzi, N.; Kim, J.-H. Dual-Color Emissive Upconversion Nanocapsules for Differential Cancer Bioimaging in Vivo. *ACS Nano* **2016**, *10*, 1512–1521.
- (14) Park, J.; Xu, M.; Li, F.; Zhou, H.-C. 3D Long-Range Triplet Migration in a Water-Stable Metal–Organic Framework for Upconversion-Based Ultralow-Power in Vivo Imaging. *J. Am. Chem. Soc.* **2018**, *140*, 5493–5499.
- (15) Amemori, S.; Sasaki, Y.; Yanai, N.; Kimizuka, N. Near-Infrared-to-Visible Photon Upconversion Sensitized by a Metal Complex with Spin-Forbidden yet Strong S<sub>0</sub>–T<sub>1</sub> Absorption. *J. Am. Chem. Soc.* **2016**, *138*, 8702–8705.
- (16) Chen, C.-H.; Tierce, N. T.; Leung, M.-K.; Chiu, T.-L.; Lin, C.-F.; Bardeen, C. J.; Lee, J.-H. Efficient Triplet–Triplet Annihilation Upconversion in an Electroluminescence Device with a Fluorescent Sensitizer and a Triplet-Diffusion Singlet-Blocking Layer. *Adv. Mater.* **2018**, *30*, e1804850.
- (17) Zhao, J.; Ji, S.; Guo, H. Triplet–Triplet Annihilation Based Upconversion: from Triplet Sensitizers and Triplet Acceptors to Upconversion Quantum Yields. *RSC Adv.* **2011**, *1*, 937–950.
- (18) Singh-Rachford, T. N.; Castellano, F. N. Triplet Sensitized Red-to-Blue Photon Upconversion. *J. Phys. Chem. Lett.* **2010**, *1*, 195–200.
- (19) Joseph, R. L. *Principles of Fluorescence Spectroscopy*; Springer Science & Business Media: New York, 2013.
- (20) Turshatov, A.; Busko, D.; Avlasevich, Y.; Miteva, T.; Landfester, K.; Baluschev, S. Synergetic Effect in Triplet–Triplet Annihilation Upconversion: Highly Efficient Multi-Chromophore Emitter. *ChemPhysChem* **2012**, *13*, 3112–3115.
- (21) Cui, X.; Charaf-Eddin, A.; Wang, J.; Le Guennic, B.; Zhao, J.; Jacquemin, D. Perylene-Derived Triplet Acceptors with Optimized Excited State Energy Levels for Triplet–Triplet Annihilation Assisted Upconversion. *J. Org. Chem.* **2014**, *79*, 2038–2048.
- (22) Cui, X.; El-Zohry, A. M.; Wang, Z.; Zhao, J.; Mohammed, O. F. Homo- or Hetero-Triplet–Triplet Annihilation? A Case Study with Perylene-BODIPY Dyads/Triads. *J. Phys. Chem. C* **2017**, *121*, 16182–16192.
- (23) Schneider, F.; Lippert, E. Electron Spectra and Electron Structure of 9,9'-Dianthryl. *Ber. Bunsen-Ges. Phys. Chem.* **1968**, *72*, 1154–1160.
- (24) Dance, Z. E. X.; Mickle, S. M.; Wilson, T. M.; Ricks, A. B.; Scott, A. M.; Ratner, M. A.; Wasielewski, M. R. Intersystem Crossing Mediated by Photoinduced Intramolecular Charge Transfer: Julolidine–Anthracene Molecules with Perpendicular  $\pi$  Systems. *J. Phys. Chem. A* **2008**, *112*, 4194–4201.
- (25) Whited, M. T.; Patel, N. M.; Roberts, S. T.; Allen, K.; Djurovich, P. I.; Bradforth, S. E.; Thompson, M. E. Symmetry-Breaking Intramolecular Charge Transfer in the Excited State of Meso-Linked BODIPY Dyads. *Chem. Commun.* **2012**, *48*, 284–286.
- (26) Wang, Z.; Zhao, J. Bodipy–Anthracene Dyads as Triplet Photosensitizers: Effect of Chromophore Orientation on Triplet-State Formation Efficiency and Application in Triplet–Triplet Annihilation Upconversion. *Org. Lett.* **2017**, *19*, 4492–4495.
- (27) Liu, Y.; Zhao, J.; Iagatti, A.; Bussotti, L.; Foggi, P.; Castellucci, E.; Di Donato, M.; Han, K.-L. A Revisit to the Orthogonal Bodipy Dimers: Experimental Evidence for the Symmetry Breaking Charge Transfer-Induced Intersystem Crossing. *J. Phys. Chem. C* **2018**, *122*, 2502–2511.
- (28) Zhao, J.; Wu, W.; Sun, J.; Guo, S. Triplet Photosensitizers: from Molecular Design to Applications. *Chem. Soc. Rev.* **2013**, *42*, 5323–5351.
- (29) Porter, G.; Windsor, M. W.; Norrish Ronald George, W. The Triplet State in Fluid Media. *Proc. R. Soc. London, Ser. A* **1958**, *245*, 238–258.
- (30) Cao, X.; Hu, B.; Zhang, P. High Upconversion Efficiency from Hetero Triplet–Triplet Annihilation in Multiacceptor Systems. *J. Phys. Chem. Lett.* **2013**, *4*, 2334–2338.
- (31) Gray, V.; Dzebo, D.; Lundin, A.; Alborzpour, J.; Abrahamsson, M.; Albinsson, B.; Moth-Poulsen, K. Photophysical Characterization of the 9,10-Disubstituted Anthracene Chromophore and Its Applications in Triplet–Triplet Annihilation Photon Upconversion. *J. Mater. Chem. C* **2015**, *3*, 11111–11121.
- (32) Yu, X.; Cao, X.; Chen, X.; Ayres, N.; Zhang, P. Triplet–Triplet Annihilation Upconversion from Rationally Designed Polymeric

Emitters with Tunable Inter-Chromophore Distances. *Chem. Commun.* **2015**, 51, 588–591.

(33) Liang, Z.-Q.; Sun, B.; Ye, C.-Q.; Wang, X.-M.; Tao, X.-T.; Wang, Q.-H.; Ding, P.; Wang, B.; Wang, J.-J. New Anthracene Derivatives as Triplet Acceptors for Efficient Green-to-Blue Low-Power Upconversion. *ChemPhysChem* **2013**, 14, 3517–3522.

(34) Balushev, S.; Yakutkin, V.; Miteva, T.; Avlasevich, Y.; Chernov, S.; Aleshchenkov, S.; Nelles, G.; Cheprakov, A.; Yasuda, A.; Müllen, K.; Wegner, G. Blue-Green Up-Conversion: Noncoherent Excitation by NIR Light. *Angew. Chem., Int. Ed.* **2007**, 46, 7693–7696.

(35) Monguzzi, A.; Mezyk, J.; Scotognella, F.; Tubino, R.; Meinardi, F. Upconversion-Induced Fluorescence in Multicomponent Systems: Steady-State Excitation Power Threshold. *Phys. Rev. B: Condens. Matter Mater. Phys.* **2008**, 78, 195112.

(36) Rettig, W. Charge Separation in Excited States of Decoupled Systems—TICT Compounds and Implications Regarding the Development of New Laser Dyes and the Primary Process of Vision and Photosynthesis. *Angew. Chem., Int. Ed. Engl.* **1986**, 25, 971–988.

(37) Grozema, F. C.; Swart, M.; Zijlstra, R. W. J.; Piet, J. J.; Siebbeles, L. D. A.; van Duijnen, P. T. QM/MM Study of the Role of the Solvent in the Formation of the Charge Separated Excited State in 9,9'-Bianthryl. *J. Am. Chem. Soc.* **2005**, 127, 11019–11028.

(38) Yao, L.; Zhang, S.; Wang, R.; Li, W.; Shen, F.; Yang, B.; Ma, Y. Highly Efficient Near-Infrared Organic Light-Emitting Diode Based on a Butterfly-Shaped Donor–Acceptor Chromophore with Strong Solid-State Fluorescence and a Large Proportion of Radiative Excitons. *Angew. Chem.* **2014**, 126, 2151–2155.